Acta Biomaterialia 166 (2023) 447–453

Contents lists available at ScienceDirect

Acta Biomaterialia

journal homepage: www.elsevier.com/locate/actbio

Full length article

Lower hardness than strength: The auxetic composite microstructure of limpet tooth

Michael Wurmshuber[a], Jana Wilmers[b,c], Jongil Kim[d], Sang Ho Oh[d,*], Swantje Bargmann[b,c,*], Daniel Kiener[a,*]

[a] Chair of Materials Physics, Department Materials Science, Montanuniversität Leoben, Austria
[b] Chair of Solid Mechanics, School of Mechanical Engineering and Safety Engineering, University of Wuppertal, Germany
[c] Wuppertal Center for Smart Materials & Systems, University of Wuppertal, Germany
[d] Department of Energy Engineering, KENTECH Institute for Energy Materials and Devices, Korea Institute of Energy Technology (KENTECH), Republic of Korea

ARTICLE INFO

Article history:
Received 13 January 2023
Revised 30 March 2023
Accepted 24 April 2023
Available online 29 April 2023

Keywords:
Biomaterials
Auxetic materials
Nanoindentation
Micromechanical modeling

ABSTRACT

The limpet tooth is widely recognized as nature's strongest material, with reported strength values up to 6.5 GPa. Recently, microscale auxeticity has been discovered in the leading part of the tooth, providing a possible explanation for this extreme strength. Utilizing micromechanical experiments, we find hardness values in nanoindentation that are lower than the respective strength observed in micropillar compression tests. Using micromechanical modeling, we show that this unique behavior is a result of local tensile strains during indentation, originating from the microscale auxeticity. As the limpet tooth lacks ductility, these tensile strains lead to microdamage in the auxetic regions of the microstructure. Consequently, indentation with a sharp indenter always probes a damaged version of the material, explaining the lower hardness and modulus values gained from nanoindentation. Micropillar tests were found to be mostly insensitive to such microdamage due to the lower applied strain and are therefore the suggested method for characterizing auxetic nanocomposites.

Statement of significance

This work explores the micromechanical properties of limpet teeth, nature's strongest biomaterial, using micropillar compression testing and nanoindentation. The limpet tooth microstructure consists of ceramic nanorods embedded in a matrix of amorphous SiO_2 and arranged in a pattern that leads to local auxetic behavior. We report lower values for nanoindentation hardness than for compressive strength, a unique behavior usually not achievable in conventional materials. Utilizing micromechanical finite element simulations, we identify the reason for this behavior to be microdamage formation resultant of the auxetic behavior, sharp indenter tip and lack of ductility of the limpet tooth microstructure. This formation of microdamage is not expected in micropillar compression tests due to lower locally imposed strain.

Introduction

Indentation hardness testing has been a staple in the evaluation and quality control of metals and other engineering materials for more than a century now, since Brinell, Ludwik and Vickers suggested their spherical, conical and pyramidal indenter shapes, respectively [1–4]. The main advantages include a fast and easy sample preparation and testing procedure and a relatively straightforward conversion from hardness to yield strength. In 1951, Tabor [2] introduced a rule of thumb stating that the hardness of a metal is about 3 times its yield strength under fully plastic conditions. The factor relating hardness and yield strength, commonly referred to as constraint factor C^*, has since then be found to not be constant, but to depend on indenter shape, indentation strain and on material properties, ranging from purely elastic ($C^* = 1.07$) to fully plastic conditions ($C^* = 2.91$) [5–7]. For self-similar indenter geometries, such as conical or Berkovich indenters, the indentation strain is constant and the constraint factor therefore only dependent on the material behavior. While there has been work on bulk

* Corresponding authors.
E-mail addresses: shoh@kentech.ac.kr (S.H. Oh), bargmann@uni-wuppertal.de (S. Bargmann), daniel.kiener@unileoben.ac.at (D. Kiener).

https://doi.org/10.1016/j.actbio.2023.04.035

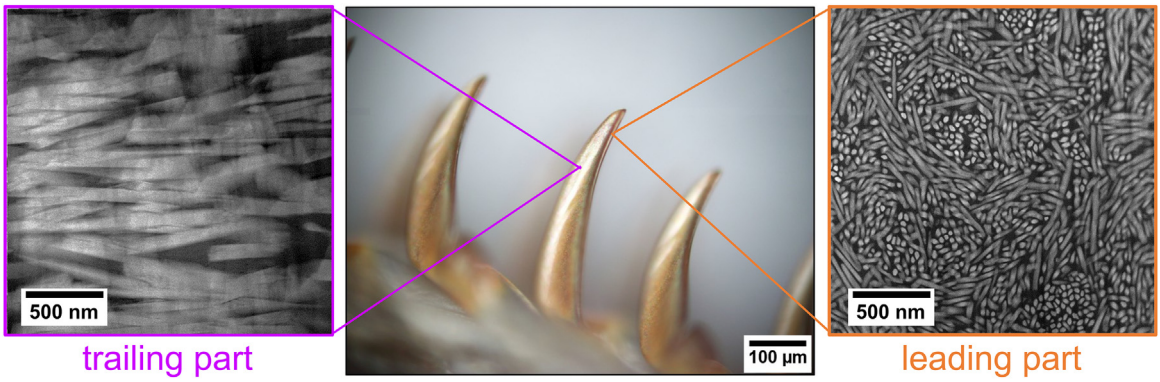

Fig. 1. Limpet tooth and annular dark-field STEM images of the microstructure in trailing and leading part.

metallic glasses exhibiting constraint factors higher than this upper bound of about 3 [8,9], to the authors' best knowledge, values lower than 1, i.e., a lower value for hardness than yield strength, have never been reported.

The teeth of limpets (*Patella vulgata*) have drawn a lot of attention in past years, since their extreme tensile strength has been reported [10,11], even outperforming spider silk as nature's strongest material [12]. These teeth consist of nanosized, defect-free goethite (α-FeOOH) rods, embedded in a matrix of hydrated silica ($SiO_2 \cdot nH_2O$) (see Fig. 1). Recently, it was discovered that bundles of nanorods can perform a rotational movement, which helps the composite to deal with high mechanical loads. Additionally, the nanorods can also rotate individually along their principal rod axis. The combination of these two rotational modes results in local auxetic behavior of the rod-matrix composite, which is believed to be the origin of the extreme strength of the leading part of the tooth [13]. In the trailing part of the tooth, where rods are larger, imperfect and not as closely spaced (Fig. 1), no rod rotation or auxetic material behavior have been observed.

In general, indentation of auxetic materials is expected to show an increased indentation resistance and therefore a higher measured hardness due to the negative Poisson ratio. This has been predicted in various simulations [14–16], which were conducted either on auxetic foam structures or purely elastic model materials and have since then sparked interest in the design of advanced auxetic (composite) materials with superior mechanical and functional properties [14,17–22].

On the contrary, investigating the strength and indentation hardness of the limpet tooth and utilizing micromechanical modeling, the present work explains that microscale auxeticity can lead to a constraint factor $C^* < 1$, thus enabling materials with a hardness lower than their yield strength.

Experiments

To investigate hardness and strength of the limpet tooth, our micropillar compression tests from [13] are investigated further and correlated to Berkovich nanoindentation experiments performed on the leading and trailing part of related limpet teeth. For that, individual limpet teeth were cut from the limpet radula and mounted in an upright position on silicon plates using epoxy resin. Subsequently, the teeth were carbon coated and the tips severed by a horizontal cut using a femtosecond laser work station (Origami 10 XP, Onefive GmbH, Regensdorf, Switzerland) [23] inside a dual-beam FIB-SEM (Zeiss Auriga, Zeiss GmbH, Oberkochen, Germany). For teeth used for nanoindentation experiments, this uncovered cross-section of the tooth was subsequently ion-polished using a FIB-SEM (Zeiss LEO 1540XB, Zeiss GmbH, Oberkochen, Germany). For micropillar compression testing, instead of the cross-section polishing, a lamella was precut using the femtosecond laser, before subsequently pillars with dimensions of about 3 × 3 × 10 µm³ were fabricated with the FIB-SEM (see Fig. 2**a**) [13].

The micropillar compression tests were performed in-situ in a scanning electron microscope (SEM; Zeiss LEO 982, Zeiss GmbH, Germany) using an UNAT-SEM indenter (Zwick GmbH & Co KG, Germany) equipped with a conductive diamond flat punch (Synton-MDP AG, Switzerland). After the tests, the recorded force-displacement data was corrected for sample compliance using the recorded in-situ images and subsequently converted to stress-strain curves using the known specimen dimensions.

Nanoindentation testing was performed on the polished tooth cross-section using a G200 Nanoindenter (KLA Corp., USA) equipped with a conductive diamond Berkovich tip (Synton-MDP AG, Switzerland) and utilizing the continuous stiffness measurement (CSM) option. The indents were performed to a maximum depth of 300 nm, thus deep enough to sample a sufficient amount of material to receive representative results and shallow enough to place a large number of indents on top of the cross-section to achieve a good spatial resolution without indents influencing each other. A total of 34 indents were placed all over the cross-section, 22 in the trailing part and 12 in the leading part.

The results from the nanoindentation and microcompression tests are depicted in Fig. 2. One can immediately see from Fig. 2c that the classic rule of thumb of Tabor does not hold for the conducted experiments. The trailing part shows a hardness of 3.00 ± 0.41 GPa and a strength of 2.55 ± 0.34 GPa, which results in a constraint factor C^* of 1.18. This is in good agreement with typical C^* values in literature for purely elastic materials [5–7]. When reviewing the stress-strain curves of the tested micropillars in Fig. 2**b**, one can see that pillars in the leading and trailing parts show such a purely elastic behavior until sudden catastrophic failure. Therefore, one would expect a similar C^* value for the leading part material. The conducted experiments, however, revealed a hardness of 1.68 ± 0.25 GPa and a strength of 3.59 ± 0.29 GPa, i.e., a significantly lower hardness than strength and a related C^* of only 0.47. A constraint factor smaller than 1 disrupts our understanding of plasticity and should not be achievable in any material. Furthermore, the leading part's hardness being lower than the trailing part's hardness contradicts the countless theoretical works [14,15] that predict a higher indentation resistance of auxetic materials. While auxeticity in the leading part has only been shown locally, the hardness is expected to be at least slightly higher than the trailing part's hardness which is non-auxetic. Moreover, the leading part also shows higher mineralization than the trailing part (see Fig. 1), which should also result in a higher hardness, as is observed for the strength values from micropillar compression tests.

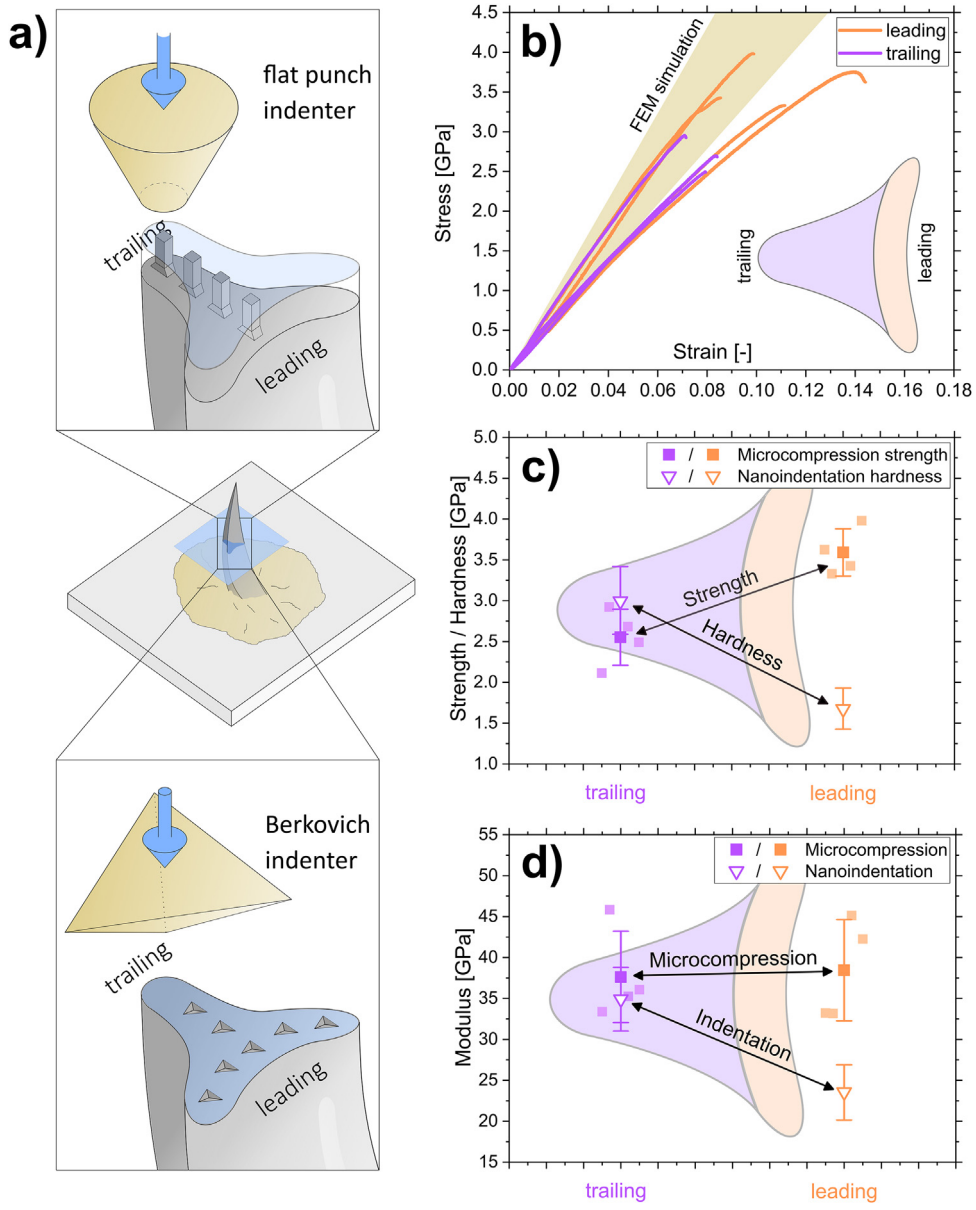

Fig. 2. Results from micropillar compression and nanoindentation tests on limpet teeth. a) Experimental test setup. b) Stress-strain curves from micropillar compression tests and linear elastic FEM simulations (yellow corridor; on the leading part only) (reproduced from [13]). c) Strength and hardness as well as d) elastic modulus values gained from both microcompression and nanoindentation experiments in trailing (non-auxetic) and leading (auxetic) part of limpet tooth.

Additionally, the elastic modulus, which averaged between 35 and 40 GPa for microcompression tests in both parts and nanoindentation in the trailing part, dropped to 23.5 ± 3.4 GPa in the indentation experiments on the leading part of the limpet tooth (Fig. 2**d**).

Micromechanical finite element modeling

To explain this unique combination of hardness and strength, we perform micromechanical simulations of the indentation process. Micromechanical modeling has successfully been employed to investigate the mechanics and microstructural dependences of different hard tissues, e.g. [13,24–27].

A representative volume element (RVE) [28] is constructed from TEM images of the limpet tooth leading part microstructure (Fig. 3**a**). The structure is approximated by a subdivision into a non-auxetic material and auxetic regions (see **Supplementary Material** for the material parameters). Both regions consist of goethite nanorods ($E_r = 225$ GPa, $\nu_r = 0.24$; both values stem from ab-initio simulations in our previous work [13]) and an amorphous hydrated silica matrix ($E_m = 8$ GPa, $\nu_m = 0.12$; [29]). The difference lies in the arrangement of these nanorods: bundles of parallel aligned nanorods (modelled as circular auxetic regions; depicted in blue in Fig. 3b) are surrounded by perpendicularly oriented nanorods (modelled as a continuous non-auxetic region; depicted in grey in Fig. 3**b**) that weave around the bundles.

The difference in the alignment of the nanorods leads to different material properties, even though both areas are made of the same two constituents. The bundles are known to act as rotation centers under loading, resulting in locally auxetic behavior [13]. Thus, its Poisson's ratio ν_{aux} is set to -0.6 to mimic the auxetic behavior. As the nanorods in the auxetic region are aligned perpendicularly to the loading direction, the Reuss estimate [30] of the homogenized elastic modulus in the auxetic regions is calculated as the weighted mean of the material properties of the goethite

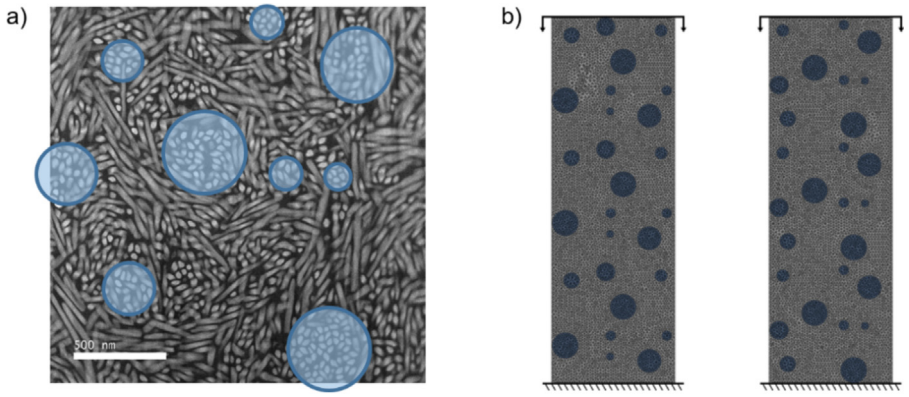

Fig. 3. Limpet tooth leading part: a) TEM image of microstructure displaying vertical bundles of nanorods that represent auxetic rotation centers. b) FEM models of two micropillars generated based on microstructure images. The auxetic regions are modelled as circular areas (blue).

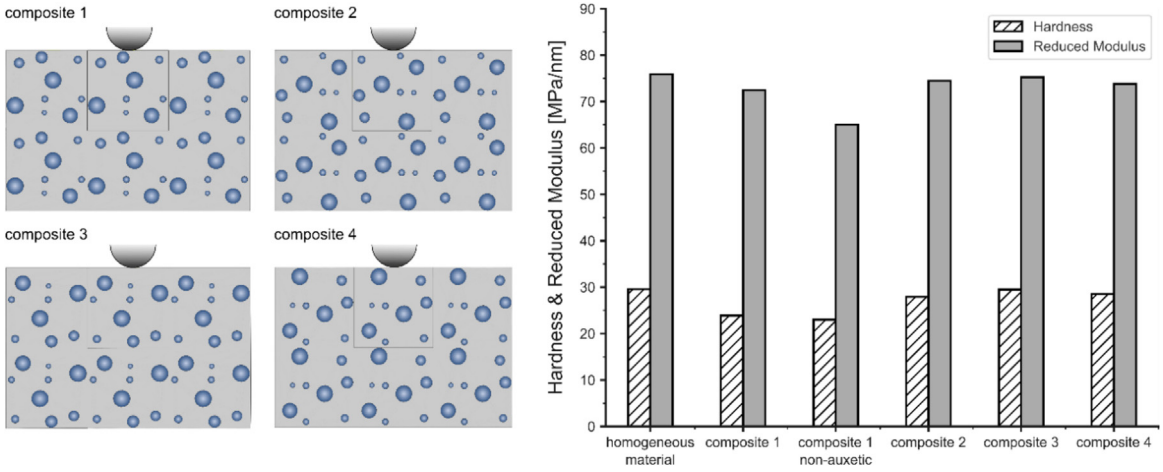

Fig. 4. Spherical indentation on microstructure models of the limpet tooth. The indentation responses of all composites show almost no deviation, also compared to a homogeneous approximation of the material without any auxeticity. Thus, auxeticity cannot be the sole reason for the difference between microcompression and nanoindentation results.

nanorods and the hydrated silica matrix:

$$E_{aux} = \frac{E_m E_r}{f_r E_m + [1 - f_r] E_r} = 15.5 \text{ GPa}.$$

From TEM images, the volume fraction of nanorods f_r has been determined to be about 50% [13].

For the non-auxetic region, a mixed Reuss-Voigt estimate [30,31] is used for the homogenized elastic modulus to account for the lower degree of alignment of the nanorods in this region

$$E_{n-aux} = 0.25[f_r E_r + [1 - f_r] E_m] + [1 - 0.25] E_{aux} = 40.7 \text{ GPa}$$

and the Poisson's ratio ν_{n-aux} is predicted by the rule of mixture $\nu_{n-aux} = f_r \nu_r + [1 - f_r]\nu_m = 0.18$.

Two micropillars with a height of 3 µm and a diameter of 1 µm (see Fig. 3b) were generated based on the RVE. Simulating compression tests on these pillars, the elastic moduli are found to be 39.62 GPa and 39.58 GPa, which is in very good agreement with the experimental results of 38.4 ± 6.2 GPa (see Fig. 2), thus, verifying the calculated material parameters. The stress peaks within the tested micropillars are found in the vicinity of the auxetic regions (**Supplementary Fig. S1**).

In addition, indentation with a spherical indenter is simulated on four composites with different microstructures based on rotations of the RVE (see Fig. 4). The indentation is modeled displacement controlled and the resulting force-per-depth of the structure is calculated for each load step. From this force-displacement response, the reduced elastic modulus is calculated following Oliver & Pharr [7,30]. All composites show a similar mechanical behavior to a hypothetical homogeneous case, where both regions consist of the same material ($E = 39.6$ GPa, $\nu = 0.18$) (Fig. 4). Thus, local auxeticity cannot be the sole reason for the difference in behavior found in microcompression and nano-indentation experiments. As will be seen in the next Section, this difference can be explained by consideration of microdamage.

Composite 1, where an auxetic region is located directly underneath the indenter, results in a slightly lower modulus. If the bundles are assumed to be non-auxetic ($\nu_{n-aux} = 0.18$) in this composite model, the modulus decreases even further, indicating that it is an effect of the microstructure, not the auxeticity. This is confirmed by the stress distributions in **Supplementary Fig. S5**.

Nanoindentation-induced microdamage

Indentation of auxetic materials results in high local tensile stresses in large regions below the indenter (compare **Supplementary Figs. S4** and **S5** and **Supplementary Material**). In combination with the inability of the limpet tooth microstructure to deform plastically, as showcased in the stress-strain curves in Fig. 2**b**, it is likely that microdamage or microcrack formation occur in the leading part microstructure during indentation. Especially sharp indenter tips, such as the Berkovich tip commonly used in nanoindentation, are known to introduce a large amount of plastic strain to the material (around 7% for the Berkovich indenter shape [2,31]).

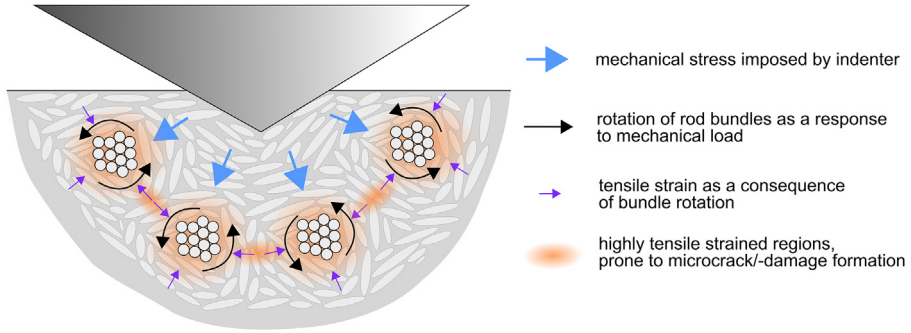

Fig. 5. Schematic of indentation on limpet tooth microstructure. Mechanical load and high strains imposed by the indenter lead to a rotational response and microscale auxeticity of the vertical nanorod bundles. This, in turn, results in highly strained regions between the bundles that are susceptible to microdamage formation, given the lack of ductility of the auxetic composite.

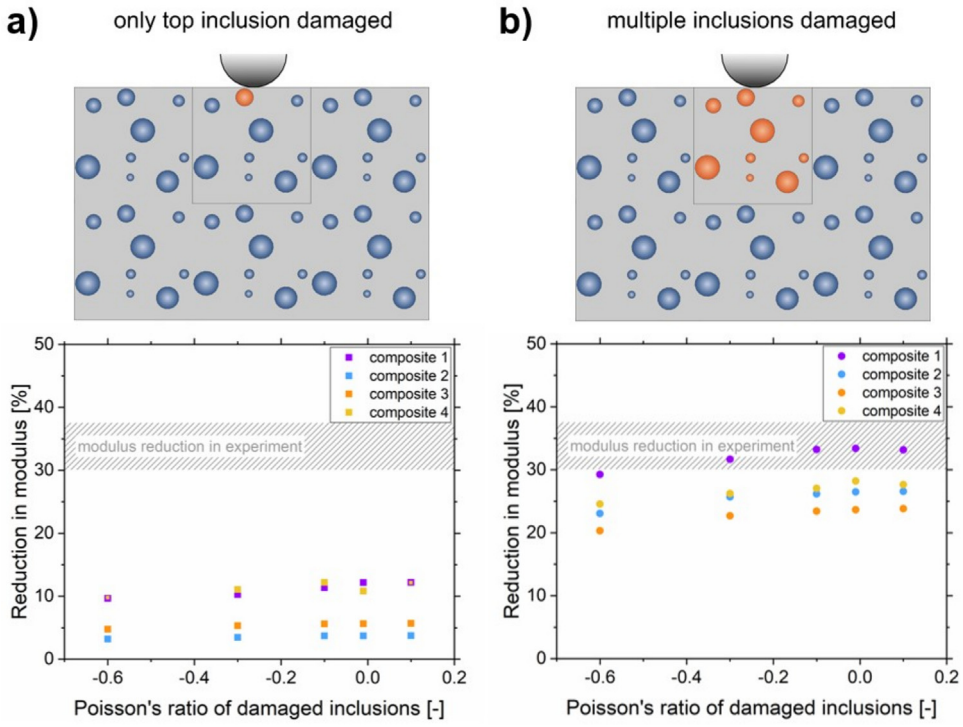

Fig. 6. Results from indentation simulations with microdamaged regions. Damage in the auxetic regions leads to a decrease in modulus in all modeled microstructures. However, only an increased amount of microdamage near the indenter can be responsible for the observed experimental modulus reduction, as seen in a comparison of the bottom left and right figures. Thus, microdamage near the indenter leads to nanoindentation measurements that (falsely) indicate lower modulus and hardness.

An illustration of the mechanisms that can lead to such formation of microdamage in the limpet tooth microstructure is depicted in Fig. 5. The stresses and strains imposed by the Berkovich indenter lead to a rotational response of the nanorod bundles. Consequently, these rotations result in tensile strains between and around the auxetic rotation centers. As the limpet tooth microstructure lacks ductility and therefore the ability to plastically deform, these strains are expected to initiate microdamage and microcrack formation in the microstructure during indentation.

While the direct experimental observation of such microdamage would be preferred, the expected size of the cracks on the nanoscale renders this a challenging endeavor. All damage will occur beneath the surface and cutting FIB trenches or performing TEM lift-outs is not feasible, as FIB debris will most likely fill up the microcracks and lift-out thinning is very prone to tearing open cracks or inhomogeneities in the microstructure. Therefore, a simulation approach is the method of choice for investigating the possibility of microdamage formation. Following these considerations, microdamage is introduced to the RVE simulations in the form of regions with a reduced elastic modulus (10% of the original value). Damage is simulated in the auxetic material in all four composites for (i) only the top most circular region and for (ii) multiple regions underneath the indenter (Fig. 6). Moreover, the Poisson's ratios of the damaged auxetic regions are varied. It can easily be imagined that microdamage, such as cracks, in the auxetic regions, can severely impede their ability to perform a rotational movement. Without such, they would lose their auxeticity and their Poisson's ratio should converge towards zero.

The reductions in the elastic moduli due to microdamage are calculated from indentation simulations of damaged composites compared to their undamaged counterparts (Fig. 6). The elastic moduli decrease in all microdamaged composites. It is logical that microstructures with more damage show a larger reduction in elastic moduli. Additionally, a trend is visible that the modulus reduction is more pronounced when the Poisson's ratio of the damaged regions approaches zero, i.e. when the composites lose their auxeticity due to microdamage.

The composites with increased damage and reduced Poisson's ratio in these damaged areas approach the experimental modulus reduction, i.e., the difference between moduli measured by micropillar compression and nanoindentation. Composites 1 and 4 show the highest modulus reduction due to microdamage, likely because they both contain a larger damaged region close to the indenter contact point. The reason why the simulations do not match the experimental results exactly might be due to the simplified microstructure, assumed perfect contact between the regions, or an underestimation of the amount of microdamage. However, the results presented in Fig. 6 strongly suggest that microdamage formation is indeed the reason as to why nanoindentation measurements on the leading part of the limpet teeth show lower hardness and elastic modulus values than compression tests and indentation on the (non-auxetic) trailing part.

Notably, when the same microdamage in the auxetic regions is modeled in the two micropillars, the moduli only decrease from 39.62 GPa to 35.54 GPa and from 39.58 GPa to 36.16 GPa, respectively. This comparably insignificant decrease in modulus of about 10% renders the pillars almost insensitive to microdamage. Moreover, the applied strain in microcompression tests is uniaxial and significantly lower compared to nanoindentation with a sharp indenter tip, which is why such microdamage is not likely to form within the micropillars in the first place.

The formation of microdamage due to the nanoindentation process itself might now raise the question as how to accurately measure the intrinsic hardness of such auxetic composites. As deduced above, the reason for the microdamage is believed to reside in the large applied plastic strains imposed by the sharp indenter tip that are translated to tensile strains through the auxetic rotational movement of nanorod bundles. Utilizing indenter tips that apply less plastic strain onto the material might therefore pose a solution. For instance, spherical indenter tips apply plastic strain proportional to the indenter displacement [7]. However, due to the inability of the limpet tooth microstructure to handle tensile strains, the strain limit to avoid microdamage might be very low. In order to impose such small strains, the spherical indenter tip can only penetrate the surface by a very shallow amount, which could lead to inaccurate hardness results influenced largely by surface roughness effects, tip imperfections or size effects. However, such experiments are planned in the future to further investigate this peculiar behavior the limpet tooth microstructure displays.

In theory, one could also assess the hardness of the limpet tooth from micropillar compression tests, if a value for the constraint factor is properly assumed. If a C^* of 1.18 is considered (as was measured for the trailing part of the limpet tooth), the hardness of the leading part would be approximately 4.25 GPa.

Conclusions

This work explored why the leading part of limpet teeth shows a lower nanoindentation hardness than strength measured in micropillar compression tests. This rather unusual behavior of a constraint factor smaller than 1 was studied extensively using finite element modeling. The limpet tooth microstructure consists of bundles of nanorods embedded in an amorphous matrix. The arrangement of these rods enables rotation under mechanical load and, as a consequence, local auxetic behavior, as shown in previous work [13]. By indentation of the composite with a sharp indenter tip, large amounts of strain are imposed on the microstructure. The local rotational auxeticity of the composite can therefore result in large tensile stresses around and in between the auxetic rotation centers, which the limpet tooth is not able to dissipate through plastic deformation. Instead, microdamage formation in these highly strained regions is likely. This behavior is in stark contrast to other gastropod teeth, such as chiton teeth. As these biocomposite materials do not exhibit auxetic regions, no tensile strains arise within the materials, making it possible to probe their extraordinary high hardness of over 10 GPa via nanoindentation [32].

By modeling microstructures including damaged auxetic regions, we showed that the elastic modulus of the material deduced from nanoindentation decreases significantly due to microdamage induced during the indentation. Additionally, near the indenter, the local auxeticity of the microstructure might get lost due to microdamage. In contrast, modeling pre-damaged micropillars resulted in negligible change of the elastic moduli compared to non-damaged pillars. Thus, by indenting the limpet tooth microstructure with a sharp indenter tip, one measures a damaged and possibly non-auxetic area of the microstructure and, consequently, a lower hardness and elastic modulus than the actual material possesses. As micropillars seem to be insensitive to such microdamage and do not impose such high strains (which would lead to microdamage) in the first place, the mechanical data and response gained from these tests can be trusted.

Statistical analysis

For the results of nanoindentation and micropillar compression experiments, a normal distribution was assumed. All presented experimental results are given as mean value and the calculated standard deviation as error.

Declaration of Competing Interest

The authors declare that they have no known competing financial interests or personal relationships that could have appeared to influence the work reported in this paper.

Acknowledgements

Funding by the European Research Council under ERC Grant 771146 (TOUGHIT) is acknowledged. The authors thank Dr. Manuel Pfeifenberger, Dr. Markus Alfreider and Dr. Alexander Leitner for their support with sample preparation and testing. Further, we are grateful for Dr. Xianglong Peng's preliminary simulations during the early developments of the work. The TEM work was supported by National Research Foundation of Korea (NRF) funded by the Korea government (MSIT) (No. NRF-2020R1A2C2101735), Creative Materials Discovery Program (NRF-2019M3D1A1078296), and, the KENTECH Research Grant (KRG2022-01-019). The TEM work at Sungkyunkwan University (SKKU) was supported by Advanced Facility Center for Quantum Technology and the TEM work at KENTECH supported by Center for Shared Research Facilities.

Supplementary materials

Supplementary material associated with this article can be found, in the online version, at doi:10.1016/j.actbio.2023.04.035.

References

[1] A.C. Fischer-Cripps, Nanoindentation (2011).
[2] D. Tabor, The Hardness of Metals, Clarendon Press, Oxford, 1951.
[3] A. Wahlberg, Brinell's method of determining hardness, J. Iron Steel Inst. 59 (1901) 243.
[4] P. Ludwik, Die Kegelprobe: Ein neues Verfahren zur Härtebestimmung von Materialien, Springer, Berlin, 1908.
[5] K.L. Johnson, The correlation of indentation experiments, J. Mech. Phys. Solids. 18 (1970) 115–126, doi:10.1016/0022-5096(70)90029-3.
[6] Y.G. Park, G.M. Pharr, Nanoindentation with spherical indenters: finite element studies of deformation in the elastic–plastic transition regime, Thin Solid Films (2003) 246–250 447–448, doi:10.1016/S0040-6090(03)01102-7.
[7] A. Leitner, V. Maier-Kiener, D. Kiener, Essential refinements of spherical nanoindentation protocols for the reliable determination of mechanical flow curves, Mater. Des. 146 (2018) 69–80, doi:10.1016/j.matdes.2018.03.003.

[8] V. Keryvin, Indentation of bulk metallic glasses: Relationships between shear bands observed around the prints and hardness, Acta Mater. 55 (2007) 2565–2578, doi:10.1016/j.actamat.2006.12.005.
[9] K.Eswar Prasad, R. Raghavan, U. Ramamurty, Temperature dependence of pressure sensitivity in a metallic glass, Scr. Mater. 57 (2007) 121–124, doi:10.1016/j.scriptamat.2007.03.033.
[10] D. Lu, A.H. Barber, Optimized nanoscale composite behaviour in limpet teeth, J. R. Soc. Interface. 9 (2012) 1318–1324, doi:10.1098/rsif.2011.0688.
[11] A.H. Barber, D. Lu, N.M. Pugno, Extreme strength observed in limpet teeth, J. R. Soc. Interface. 12 (2015) 20141326–20141326, doi:10.1098/rsif.2014.1326.
[12] S. Keten, Z. Xu, B. Ihle, M.J. Buehler, Nanoconfinement controls stiffness, strength and mechanical toughness of B-sheet crystals in silk, Nat. Mater. 9 (2010) 359–367, doi:10.1038/nmat2704.
[13] S.H. Oh, J.-K. Kim, Y. Liu, M. Wurmshuber, X.-L. Peng, J. Seo, J. Jeong, Z. Wang, J. Wilmers, C. Soyarslan, J. Kim, B. Kittiwirayanon, J. Jeong, H.-J. Kim, Y.H. Huh, D. Kiener, S. Bargmann, H. Gao, Limpet teeth microstructure unites auxeticity with extreme strength and high stiffness, Sci. Adv. 8 (2022) eadd4644, doi:10.1126/sciadv.add4644.
[14] C. Huang, L. Chen, Negative Poisson's ratio in modern functional materials, Adv. Mater. 28 (2016) 8079–8096, doi:10.1002/adma.201601363.
[15] D. Photiou, N. Prastiti, E. Sarris, G. Constantinides, On the conical indentation response of elastic auxetic materials : effects of Poisson's ratio, contact friction and cone angle, Int. J. Solids Struct. 81 (2016) 33–42, doi:10.1016/j.ijsolstr.2015.10.020.
[16] N. Chan, K.E. Evans, Indentation resilience of conventional and auxetic foams, J. Cell. Plast. 34 (1998) 231–260, doi:10.1177/0021955X9803400304.
[17] R.S. Lakes, Design considerations for materials with negative poisson's ratios, J. Mech. Des. Trans. ASME. 115 (1993) 696–700, doi:10.1115/1.2919256.
[18] R. Lakes, Advances in negative Poisson's ratio materials, Adv. Mater. 5 (1993) 293–296, doi:10.1002/adma.19930050416.
[19] E. Pasternak, A.V. Dyskin, Materials and structures with macroscopic negative Poisson's ratio, Int. J. Eng. Sci. 52 (2012) 103–114, doi:10.1016/j.ijengsci.2011.11.006.
[20] H. Zhou, K. Jia, X. Wang, M.X. Xiong, Y. Wang, Experimental and numerical investigation of low velocity impact response of foam concrete filled auxetic honeycombs, Thin-Walled Struct. 154 (2020) 106898, doi:10.1016/j.tws.2020.106898.
[21] X.G. Zhang, W. Jiang, Y. Zhang, C. Luo, X.Y. Zhang, D. Han, J. Hao, X.C. Teng, Y.M. Xie, X. Ren, Energy absorption properties of composite tubes with hexagonal and re-entrant honeycomb fillers, Constr. Build. Mater. 356 (2022) 129298, doi:10.1016/j.conbuildmat.2022.129298.
[22] X.L. Peng, S. Bargmann, A novel hybrid-honeycomb structure: enhanced stiffness, tunable auxeticity and negative thermal expansion, Int. J. Mech. Sci. 190 (2021) 106021, doi:10.1016/j.ijmecsci.2020.106021.
[23] M.J. Pfeifenberger, M. Mangang, S. Wurster, J. Reiser, A. Hohenwarter, W. Pfleging, D. Kiener, R. Pippan, The use of femtosecond laser ablation as a novel tool for rapid micro-mechanical sample preparation, Mater. Des. 121 (2017) 109–118, doi:10.1016/j.matdes.2017.02.012.
[24] S. Bargmann, I. Scheider, T. Xiao, E. Yilmaz, G.A. Schneider, N. Huber, Towards bio-inspired engineering materials: modeling and simulation of the mechanical behavior of hierarchical bovine dental structure, Comput. Mater. Sci. 79 (2013) 390–401, doi:10.1016/j.commatsci.2013.06.028.
[25] X.L. Peng, S. Lee, J. Wilmers, S.H. Oh, S. Bargmann, Orientation-dependent micromechanical behavior of nacre: In situ TEM experiments and finite element simulations, Acta Biomater. 147 (2022) 120–128, doi:10.1016/j.actbio.2022.05.033.
[26] B. Bar-On, H.Daniel Wagner, Effective moduli of multi-scale composites, Compos. Sci. Technol. 72 (2012) 566–573, doi:10.1016/j.compscitech.2011.12.017.
[27] J.W. Pro, F. Barthelat, Discrete element models of tooth enamel, a complex three-dimensional biological composite, Acta Biomater. 94 (2019) 536–552, doi:10.1016/j.actbio.2019.04.058.
[28] S. Bargmann, B. Klusemann, J. Markmann, J.E. Schnabel, K. Schneider, C. Soyarslan, J. Wilmers, Generation of 3D representative volume elements for heterogeneous materials: a review, Prog. Mater. Sci. 96 (2018) 322–384, doi:10.1016/j.pmatsci.2018.02.003.
[29] A.B. Rinkevich, D.V. Perov, M.I. Samoilovich, S.M. Kleshcheva, Elastic properties and heat capacity of opal matrices and related 3D-nanocomposite materials, Phys. Solid State. 52 (2010) 2570–2576, doi:10.1134/S1063783410120218.
[30] W.C. Oliver, G.M. Pharr, An improved technique for determining hardness and elastic modulus using load and displacement sensing indentation experiments, J. Mater. Res. 7 (1992) 1564–1583, doi:10.1557/JMR.1992.1564.
[31] A. Leitner, V. Maier-Kiener, D. Kiener, Extraction of flow behavior and Hall–Petch parameters using a nanoindentation multiple sharp tip approach, Adv. Eng. Mater. (2017) 19, doi:10.1002/adem.201600669.
[32] J.C. Weaver, Q. Wang, A. Miserez, A. Tantuccio, R. Stromberg, K.N. Bozhilov, P. Maxwell, R. Nay, S.T. Heier, E. Dimasi, D. Kisailus, Analysis of an ultra hard magnetic biomineral in chiton radular teeth Recent analyses of the ultrastructural and mechanical properties of, Mater. Today 13 (2010) 42–52, doi:10.1016/S1369-7021(10)70016-X.